

Accepted Manuscript

In situ study starch gelatinization under ultra-high hydrostatic pressure using synchrotron SAXS

Zhi Yang, Qinfen Gu, Elisa Lam, Feng Tian, Sahraoui Chaieb, Yacine Hemar



PII: S0268-005X(15)30174-0

DOI: [10.1016/j.foodhyd.2015.12.007](https://doi.org/10.1016/j.foodhyd.2015.12.007)

Reference: FOOHYD 3222

To appear in: *Food Hydrocolloids*

Received Date: 23 September 2015

Revised Date: 1 December 2015

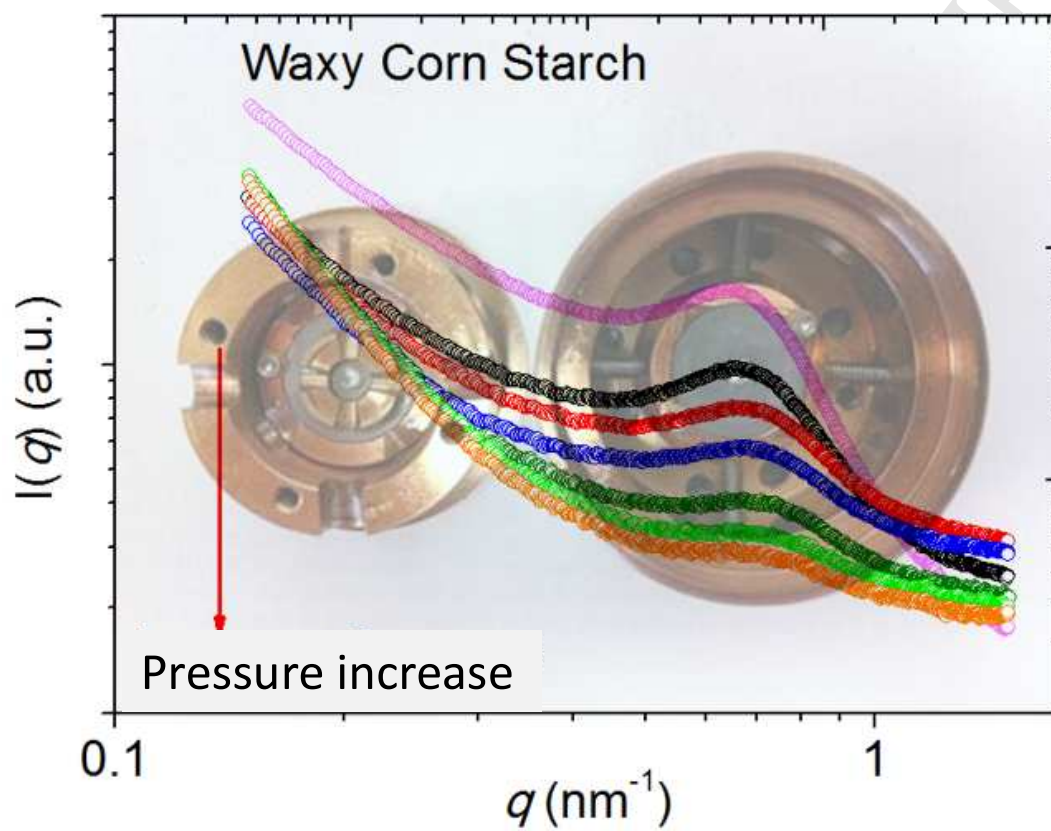
Accepted Date: 9 December 2015

Please cite this article as: Yang, Z., Gu, Q., Lam, E., Tian, F., Chaieb, S., Hemar, Y., *In situ* study starch gelatinization under ultra-high hydrostatic pressure using synchrotron SAXS, *Food Hydrocolloids* (2016), doi: 10.1016/j.foodhyd.2015.12.007.

This is a PDF file of an unedited manuscript that has been accepted for publication. As a service to our customers we are providing this early version of the manuscript. The manuscript will undergo copyediting, typesetting, and review of the resulting proof before it is published in its final form. Please note that during the production process errors may be discovered which could affect the content, and all legal disclaimers that apply to the journal pertain.

Graphical abstract

In situ synchrotron SAXS patterns of waxy corn starch under different pressure conditions. The background is a picture of the diamond anvil cell (DAC) used in this study.



1 ***In situ* study starch gelatinization under ultra-high hydrostatic pressure**
2 **using synchrotron SAXS**

3
4
5 Zhi Yang¹, Qinfen Gu², Elisa Lam¹, Feng Tian³, Sahraoui Chaieb⁴, and Yacine Hemar^{1, 5*}
6
7
8
9

10 1. School of Chemical Sciences, The University of Auckland, Private Bag 92019,
11 Auckland 1142, New Zealand.

12
13
14 2. Australian Synchrotron, 800 Blackburn Rd., Clayton 3168, Australia
15

16 3. Shanghai Synchrotron Radiation Facility, Shanghai Institute of Applied Physics, Chinese Academy
17 of Sciences, Shanghai 201204, China.
18

19 4. Division of Physical Sciences and Engineering, King Abdullah University of Science and
20 Technology (KAUST), Thuwal 23955-6900, Kingdom of Saudi Arabia.
21

22 5. The Riddet Institute, Palmerston North, New Zealand.
23
24
25
26
27
28
29
30

31 *Author to whom correspondence should be addressed: Email: y.hemar@auckland.ac.nz
32
33

34

35

36

37 **Abstract**

38 The gelatinization of waxy (very low amylose) corn and potato starches by high hydrostatic
39 pressure (HHP) (up to ~1 GPa) was investigated *in situ* using synchrotron small-angle X-ray
40 scattering (SAXS) on samples held in a diamond anvil cell (DAC). The starch pastes, made
41 by mixing starch and water in a 1:1 ratio (by weight), were pressurized and measured at room
42 temperature. During HHP, both SAXS peak areas (corresponding to the lamellar phase) of
43 waxy corn and potato starches decreased suggesting the starch gelatinization increases with
44 increasing pressure. As pressure increased, lamellar peak broadened and the power law
45 exponent increased in low q region. 1D linear correlation function was further employed to
46 analyse SAXS data. For both waxy potato and waxy corn starches, the long period length and
47 the average thickness of amorphous layers decreased when the pressure increased. While for
48 both of waxy starches, the thickness of the crystalline layer first increased, then decreased
49 when the pressure increased. The former is probably due to the out-phasing of starch
50 molecules, and the latter is due to the water penetrating into the crystalline region during
51 gelatinization and to pressure induced compression.

52

53

54

55 **Keywords:**

56 Waxy corn and potato starches; High pressure; Synchrotron small-angle X-ray scattering;

57 Diamond anvil cell

58

59

60 **1. Introduction**

61

62 Starch is one of the most common biomacromolecules present in nature and consists of two
63 major types of α -glucans at the molecular level: the linear amylose and the branched
64 amylopectin. The former is mostly linear with few branches and a molecular weight of 10^5 -
65 10^6 Da, and the latter is extensively branched with about 5-6% branches scattered along the
66 backbones with a molecular weight in the range of 10^7 - 10^9 Da (Buléon, Colonna, Planchot &
67 Ball, 1998; Pérez & Bertoft, 2010; Zobel, 1988). The starch granules display a hierarchical
68 structure periodicity and are organised into concentric rings radiating out from the central
69 hilum to the surface of the granule. The number and size of the rings depend on the botanical
70 origin of the starch, and it is generally believed to display an onion like organization with
71 alternating 120-400 nm thick amorphous and semi-crystalline growth rings (Chen, Yu, Simon,
72 Liu, Dean & Chen, 2011; Vermeulen, Derycke, Delcour, Goderis, Reynaers & Koch, 2006).
73 It is believed that the amorphous rings consist of amylose and amylopectin in a disordered
74 conformation, whereas the semi-crystalline rings are formed by a lamellar structure of
75 alternating crystalline and amorphous regions with regular repeat distance of 9-10 nm as
76 revealed by small angle x-ray scattering (SAXS) (Cameron & Donald, 1992).

77

78 Gelatinization is one of the most important processes in the industrial application of starch.
79 Besides heating starch in water, high hydrostatic pressure (HHP) can also be employed to
80 gelatinize starch (Katopo, Song & Jane, 2002; Oh, Pinder, Hemar, Anema & Wong, 2008). It
81 is suggested that during HHP, the transition of starch crystalline structures could occur (e.g.
82 from A-type to B-type) (Katopo, Song & Jane, 2002). When enough high pressure is exerted,
83 the starch granule can be fully gelatinized and loose its crystalline structures (Yang, Gu &
84 Hemar, 2013). Besides the crystalline structure changes induced by HHP, the other
85 supramolecular structures (e.g. lamellae characteristics, fractal structures, etc.) are expected
86 to be affected by HHP. Unfortunately until very recently, studies on the *in situ* effects of HHP
87 on starch systems are scarce (Gebhardt, Hanfland, Mezouar & Riekkel, 2007; Yang, Gu &
88 Hemar, 2013). Gebhardt et al. (2007) employed synchrotron SAXS/WAXS to study *in situ*
89 potato starch gelatinization under HHP, and showed that the onset of gelatinization starts with
90 the hydration of the semicrystalline lamellae and lateral breakdown of the crystalline domain.
91 The SAXS analysis in their study did not investigate the changes in the amorphous and

92 crystalline layers. Yang et al. (2013) utilised synchrotron X-ray powder diffraction (WAXS)
93 to investigate *in situ* waxy and high amylose corn starch gelatinization under HHP focusing
94 on their crystalline structure changes (e.g. crystalline type and *d*-spacing) and demonstrated
95 that starch retrogradation starts immediately after pressure removal.

96

97 In this study, synchrotron SAXS is used to probe *in situ* the effect of HHP on the structure of
98 waxy corn and potato starches. Synchrotron SAXS has the advantages over lab-bench SAXS,
99 due to its higher intensity and collimation, enabling data to be obtained in real-time, and
100 waxy starches were selected as they show clearly a peak corresponding to the lamellar phase.
101 To the best of our knowledge, this study is the first to report *in situ* synchrotron SAXS
102 measurements on waxy starch dispersions in water under high pressure using a diamond anvil
103 cell (DAC) in order to probe the changes in waxy starch amorphous and crystalline layers
104 under HHP.

105

106 **2. Materials and Methods**

107

108 **2.1 Materials and sample preparation**

109

110 Waxy maize (amylose content 1.37 ± 0.09 w/w%) and potato (amylose content 1.69 ± 0.64
111 w/w%) starches were donated by Avebe Food (Auckland, New Zealand). Starch powder (0.2
112 g) was mixed with 1 ml Milli-Q water at room temperature and vortexed for 3 min. The
113 starch suspensions were centrifuged at 10,000 rpm for 5 min and the supernatants were
114 removed. The water content in the starch paste was $\sim 50\%$ (w/w).

115

116 **2.2 Methods**

117

118 A diamond anvil cell (DAC) (easyLab) with 1 mm anvil culet size was used. The drilled hole
119 (500 μm diameter and 150 μm thickness) of stainless steel gasket was used to host the starch
120 sample and ruby balls of *ca.* 20 μm diameters were loaded with the sample to measure the
121 pressure. The pressure was generated by tightening the four cap screws of the DAC step by
122 step. The pressure was measured from the shift of the ruby fluorescence using Ocean optics
123 system (FL, USA).

124

125 *In situ* synchrotron small angle X ray scattering (SAXS) experiments were conducted on the
 126 beamline BL16B1 at the Shanghai Synchrotron Radiation Facility (SSRF, China). A
 127 monochromatic beam of 0.1240 nm wavelength was used, and the sample-to-detector
 128 distance was set to 2150 mm. Scattering was detected in the q ranges of 0.15-1.5 nm⁻¹ in
 129 which $q = (4\pi \sin \theta) / \lambda$ (where 2θ is the scattering angle and λ is the wavelength). FIT2D
 130 software (<http://www.esrf.fr/computing/scientific/FIT2D/>) was used to convert the one-
 131 dimensional (1D) data from the 2D scattering pattern. All the data were background
 132 subtracted and normalized.

133

134 2.3 Analysis of SAXS data

135

136 SAXS scattering curve were fitted to a power-law function plus a Gaussian peak (Blazek &
 137 Gilbert, 2010):

$$I(q) = B + Pq^{-\alpha} + \frac{A\sqrt{\ln 2}}{W\sqrt{\pi/4}} \exp\left(-\frac{4 \ln 2 (q - q_0)^2}{W^2}\right) \quad (1)$$

138

139 where B is the background; the second term is the power-law function where P is the power
 140 law pre-factor and α is the power-law exponent; the third term is a Gaussian function where A
 141 is the Gaussian peak area, W (nm⁻¹) the full width at half maximum of the peak, and q_0 (nm⁻¹)
 142 is the peak centre position.

143

144 The SAXS data are also analysed by the 1D linear correlation function $L(r)$ which is derived
 145 from Fourier transition of the scattering curves (Fan, et al., 2014; Zhang, et al., 2015).

146

$$r(z) = \frac{\int_0^\infty I(q)q^2 \cos(qz) dq}{\int_0^\infty I(q)q^2 dq} \quad (2)$$

147

148 In equation (2), r (nm) is the distance in real space. Determinations of the lamellar parameters
 149 of starch samples are conducted as follows: long period (d), i.e. the lamellar repeat distance is
 150 the value of z at the second maximum of $r(z)$; the average thickness of the amorphous
 151 lamellae is expressed as d_a , which can be acquired by the solution of the linear region and the
 152 flat $r(z)$ minimum. Thus, d_c , the average thickness of crystalline lamellae can be calculated

153 by $d_c = d - d_a$. The correlation function analysis was conducted using S programme package (Li,
154 2013).

155

156 **3. Results and Discussion**

157

158 *In situ* SAXS patterns of waxy corn and potato starches, under HHP, are reported in
159 Figure.1A and B, respectively. The curves are all characterized by intense scattering at low
160 scattering vector (q). A typical SAXS peak could be observed at a q of 0.6 to 0.7 nm^{-1} ,
161 indicating a 9-10 nm semi-crystalline structure, according to Bragg's law $d = 2\pi/q$ (Blazek &
162 Gilbert, 2011). HHP treatment resulted in the reduction in the peak intensity after
163 normalization. To analyse the SAXS curves Equation. (1) is used and the goodness of the fits
164 can be seen in the supporting Figures. S1 and S2. The resulting parameters are reported in
165 Figure. 2A-F. For both starches, the peak area, which indicates the degree of lamellae
166 ordering (Pikus, 2005), decreases with increase in pressure due to gelatinisation. Conversely,
167 the peak width which depends on the regularity of the lamellar arrangement within starch
168 granule (Blazek & Gilbert, 2010), increases with the increase in pressure. It could be due to
169 the fact that at the limit of lamellae compression, excess compression may be accommodated
170 by lamellar 'buckling'. This leads to an increase of the distribution of lamellar sizes thus
171 broadening the SAXS peak. A similar SAXS peak broadening has been suggested to occur
172 due to compression induced by water freezing (Perry & Donald, 2000). In the low- q region
173 the curves comply with a simple power law equation ($I(q) \sim q^{-\alpha}$) (Martin & Hurd, 1987);
174 where the exponent α gives insight into the surface/mass fractal structure of the starch
175 granules (Suzuki, Chiba & Yarno, 1997). Moreover, the mass fractal dimension ($0 < \alpha < 3$) is
176 used to indicate the compactness, whereas the surface fractal dimension ($3 < \alpha < 4$) is regarded
177 as an indicator of the degree of smoothness of the scattering objects (Zhang, et al., 2014). In
178 the case of the fractal dimension of the two starches under HHP, the mass fractal dimension
179 ($1 < \alpha < 3$) increased suggesting that the starch structures become more compact due to
180 compression during pressurization. Note that for waxy corn starch, when the pressure is
181 increased to ≥ 670 MPa, the value of α is higher than 3; suggesting the appearance of surface
182 fractal structure. It is suggested that the scattering objects of surface fractals are more
183 compact than those of mass fractals (Zhang, et al., 2014).

184

185 Further analysis of the SAXS measurements were performed using the linear correlation
186 functions (Equation (2)) (Figure. 1C-D). The most relevant morphological parameters

187 obtained through correlation function analysis are d (long period distance), d_a (average
188 thickness of amorphous layers), and d_c (crystalline and amorphous layer thickness)
189 (Figure .2D-F). For both waxy corn and potato starch, d decreases with the pressure increase.
190 This is due to lamellae compression under high pressure (Gebhardt, Hanfland, Mezouar, &
191 Riekkel, 2007). Compared to waxy corn starch, the decrease of d with pressure (up to 750 MPa)
192 is less for potato starch compared to corn starch. It is suggested that having longer
193 amylopectin chains, B-type starch (waxy potato) is much less compressible compared to A-
194 type starch (waxy corn), since lamellae phases made of long amylopectin chains require an
195 overall layer bending to accommodate the internal stresses generated by the compression
196 (Daniels & Donald, 2003; Lan, Li, Xie & Wang, 2015). As pressure is increased, the
197 amorphous layer starts to decrease for both starches probably due to simple compression
198 (Gebhardt, Hanfland, Mezouar & Riekkel, 2007) or/and due to the leaching out of starch
199 molecule from the amorphous layer (Zhang et al., 2015). Similar trend is also observed in
200 thermal gelatinization of starch (Jenkins & Donald, 1998; Zhang et al., 2015). Further, the
201 amorphous regions of starch granules may be expected to act as ‘shock absorbers’ upon the
202 application of compressive forces (Morgan, Furneaux & Larsen, 1995; Perry & Donald,
203 2000). This is also consistent with the idea that amorphous regions within lamellar systems
204 ‘protect’ the crystalline regions by preferential compression upon impact. The crystalline
205 layer thickness d_c of both waxy corn and potato are falling in the range of 5-7 nm, as
206 suggested by Putaux, Molina-Boisseau, Momaour & Dufresne, 2003. Contrary to the
207 amorphous layers, the thickness layers thickness d_c initially increased slightly followed by a
208 decrease in very high pressure region for both waxy corn and waxy potato starches.
209 Compared to the amorphous layers, the crystalline layers have higher degree of order and
210 rigidity thus are expected to be more resistant to compression (Perry & Donald, 2000).
211 During gelatinization, the water penetrates into crystalline region, which results in an increase
212 of the d_c and eventually the formation of a disordered phase through disruption of the helical
213 packing (Gebhardt, Hanfland, Mezouar & Riekkel, 2007). The decrease of d_c at very high
214 pressure could attribute to the crystalline layer compression.

215

216 Overall, in our view an important observation from these experiments is the fact that all the
217 parameters considered through the analysis of both the SAXS data and their corresponding
218 correlation functions are affected by pressure. While most of the published literature gives a
219 threshold pressure for starch gelatinisation, depending on the starch type and amylose content
220 (Buckow, Jankowiak, Knorr, & Versteeg, 2009), this study indicates that the starch granule

221 fine structure is affected as soon as pressure is applied. In all cases, this study demonstrates
222 the potential of using synchrotron SAXS in combination with a DAC to monitor *in situ* starch
223 gelatinization under HHP.

224

225 **Acknowledgements**

226 We would like to thank Dr. Fang Hong HPSTAR (Centre for High Pressure Science and
227 Technology Advanced Research, Shanghai) for facilitating our access to ruby fluorescence
228 system.

229

230

231

232 **References:**

233 Blazek, J., & Gilbert, E. P. (2010). Effect of enzymatic hydrolysis on native starch granule structure.
234 *Biomacromolecules*, 11(12), 3275-3289.

235 Blazek, J., & Gilbert, E. P. (2011). Application of small-angle X-ray and neutron scattering
236 techniques to the characterisation of starch structure: A review. *Carbohydrate Polymers*, 85(2), 281-
237 293.

238 Buléon, A., Colonna, P., Planchot, V., & Ball, S. (1998). Starch granules: structure and biosynthesis.
239 *International Journal of Biological Macromolecules*, 23(2), 85-112.

240 Buckow, R., Jankowiak, L., Knorr, D., & Versteeg, C. (2009). Pressure-temperature phase diagrams
241 of maize starches with different amylose contents. *Journal of Agricultural and Food Chemistry*,
242 57(24), 11510-11516.

243

244 Cameron, R. E., & Donald, A. M. (1992). A small-angle X-ray scattering study of the annealing and
245 gelatinization of starch. *Polymer*, 33(12), 2628-2635.

246 Chen, P., Yu, L., Simon, G. P., Liu, X., Dean, K., & Chen, L. (2011). Internal structures and phase-
247 transitions of starch granules during gelatinization. *Carbohydrate Polymers*, 83(4), 1975-1983.

248 Daniels, D. R., & Donald, A. M. (2003). An improved model for analyzing the small angle x-ray
249 scattering of starch granules. *Biopolymers*, 69(2), 165-175.

250 Fan, D., Wang, L., Chen, W., Ma, S., Ma, W., Liu, X., Zhao, J., & Zhang, H. (2014). Effect of
251 microwave on lamellar parameters of rice starch through small-angle X-ray scattering. *Food*
252 *Hydrocolloids*, 35(0), 620-626.

253 Gebhardt, R., Hanfland, M., Mezouar, M., & Riekkel, C. (2007). High-pressure potato starch granule
254 gelatinization: synchrotron radiation micro-SAXS/WAXS using a diamond anvil cell.
255 *Biomacromolecules*, 8(7), 2092-2097.

256 Jenkins, P. J., & Donald, A. M. (1998). Gelatinisation of starch: A combined SAXS/WAXS/DSC and
257 SANS study. *Carbohydrate research*, 308(1), 133-147.

258 Katopo, H., Song, Y., & Jane, J.-I. (2002). Effect and mechanism of ultrahigh hydrostatic pressure on
259 the structure and properties of starches. *Carbohydrate Polymers*, 47(3), 233-244.

- 260 Li, Z.-H. (2013). A program for SAXS data processing and analysis. *Chinese Phys. C*, 37(10), 110-115.
261
- 262 Lan, X., Li, Y., Xie, S., & Wang, Z. (2015). Ultrastructure of underutilized tuber starches and its
263 relation to physicochemical properties. *Food Chemistry*, 188, 632-640.
264
- 265 Martin, J. E., & Hurd, A. (1987). Scattering from fractals. *Journal of applied crystallography*, 20(2),
266 61-78.
- 267 Morgan, K. R., Furneaux, R. H., & Larsen, N. G. (1995). Solid-state NMR studies on the structure of
268 starch granules. *Carbohydrate research*, 276(2), 387-399.
- 269 Oh, H., Pinder, D., Hemar, Y., Anema, S., & Wong, M. (2008). Effect of high-pressure treatment on
270 various starch-in-water suspensions. *Food Hydrocolloids*, 22(1), 150-155.
- 271 Pérez, S., & Bertoft, E. (2010). The molecular structures of starch components and their contribution
272 to the architecture of starch granules: A comprehensive review. *Starch - Stärke*, 62(8), 389-420.
- 273 Perry, P., & Donald, A. (2000). The effects of low temperatures on starch granule structure. *Polymer*,
274 41(16), 6361-6373.
- 275 Pikus, S. (2005). Small-angle X-ray scattering (SAXS) studies of the structure of starch and starch
276 products. *Fibres and Textiles in Eastern Europe*, 13(5), 82-86.
- 277 Putaux, J.-L., Molina-Boisseau, S., Momaour, T., & Dufresne, A. (2003). Platelet nanocrystals
278 resulting from the disruption of waxy maize starch granules by acid hydrolysis. *Biomacromolecules*,
279 4(5), 1198-1202.
- 280 Suzuki, T., Chiba, A., & Yano, T. (1997). Interpretation of small angle X-ray scattering from starch
281 on the basis of fractals. *Carbohydrate Polymers*, 34(4), 357-363.
- 282 Vermeylen, R., Derycke, V., Delcour, J. A., Goderis, B., Reynaers, H., & Koch, M. H. J. (2006).
283 Gelatinization of starch in excess water: Beyond the melting of lamellar crystallites. A Combined
284 Wide- and Small-Angle X-ray Scattering Study. *Biomacromolecules*, 7(9), 2624-2630.
- 285 Yang, Z., Gu, Q., & Hemar, Y. (2013). In situ study of maize starch gelatinization under ultra-high
286 hydrostatic pressure using X-ray diffraction. *Carbohydrate Polymers*, 97(1), 235-238.
- 287 Zhang, B., Chen, L., Xie, F., Li, X., Truss, R. W., Halley, P. J., Shamshina, J. L., Rogers, R. D., &
288 McNally, T. (2015). Understanding the structural disorganization of starch in water-ionic liquid
289 solutions. *Physical Chemistry Chemical Physics*, 17(21), 13860-13871.
- 290 Zobel, H. (1988). Molecules to granules: A comprehensive starch review. *Starch - Stärke*, 40(2), 44-
291 50.
- 292
- 293
- 294
- 295
- 296

Highlights

- *In situ* SAXS is performed on starch dispersions under pressures of up to ~ 1 GPa.
- The starch granule fine structure is affected as soon as a pressure is applied.
- Waxy corn and potato starches showed similar structure changes due to pressure.